Room-Temperature Phosphorescence and Energy Transfer in Luminescent Multinuclear Platinum(II) Complexes of Branched Alkynyls

Chi-Hang Tao, Nianyong Zhu, and Vivian Wing-Wah Yam*[a]

Abstract: A series of luminescent branched platinum(II) alkynyl complexes, [1,3,5-{RC≡C(PEt$_3$)$_2$PtC≡C-C$_6$H$_4$C≡C}$_3$C$_6$H$_3$] (R = C$_6$H$_5$, C$_6$H$_4$OMe, C$_6$H$_4$Me, C$_6$H$_4$CF$_3$, C$_5$H$_4$N, C$_6$H$_4$SAc, 1-napthyl (Np), 1-pyrenyl (Pyr), 1-anthryl-8-ethynyl (HC≡CAn)), [1,3-{PyrC≡C(PEt$_3$)$_2$PtC≡CC$_6$H$_4$C≡C}$_2$-5-{(*i*Pr)$_3$SiC≡C}C$_6$H$_3$], and [1,3-{PyrC≡C-(PEt$_3$)$_2$PtC≡CC$_6$H$_4$C≡C}$_2$-5-(HC≡C)-C$_6$H$_3$], was successfully synthesized by using the precursors [1,3,5-{Cl(PEt$_3$)$_2$PtC≡CC$_6$H$_4$C≡C}$_3$C$_6$H$_3$] or [1,3-{Cl(PEt$_3$)$_2$PtC≡CC$_6$H$_4$C≡C}$_2$-5-{(*i*Pr)$_3$SiC≡C}C$_6$H$_3$]. The X-ray crystal structures of [1,3,5-{MeOC$_6$H$_4$C≡C-(PEt$_3$)$_2$PtC≡CC$_6$H$_4$C≡C}$_3$C$_6$H$_3$] and [1,8-{Cl(PEt$_3$)$_2$PtC≡C}$_2$An] have been determined. These complexes were found to show long-lived emission in both solution and solid-state phases at room temperature. The emission origin of the branched complexes [1,3,5-{RC≡C(PEt$_3$)$_2$PtC≡CC$_6$H$_4$C≡C}$_3$C$_6$H$_3$] with R = C$_6$H$_5$, C$_6$H$_4$OMe, C$_6$H$_4$Me, C$_6$H$_4$CF$_3$, C$_5$H$_4$N, and C$_6$H$_4$SAc was tentatively assigned to be derived from triplet states of predominantly intraligand (IL) character with some mixing of metal-to-ligand charge-transfer (MLCT) (dπ(Pt)→π*(C≡CR)) character, while the emission origin of the branched complexes with polyaromatic alkynyl ligands, [1,3,5-{RC≡C-(PEt$_3$)$_2$PtC≡CC$_6$H$_4$C≡C}$_3$C$_6$H$_3$] with R = Np, Pyr, or HC≡CAn, [1,3-{PyrC≡C-(PEt$_3$)$_2$PtC≡CC$_6$H$_4$C≡C}$_2$-5-{(*i*Pr)$_3$SiC≡C}C$_6$H$_3$], [1,3-{PyrC≡C(PEt$_3$)$_2$PtC≡C-C$_6$H$_4$C≡C}$_2$-5-(HC≡C)C$_6$H$_3$], and [1,8-{Cl(PEt$_3$)$_2$PtC≡C}$_2$An], was tentatively assigned to be derived from the predominantly ^{3}IL states of the respective polyaromatic alkynyl ligands, mixed with some ^{3}MLCT (dπ(Pt)→π*(C≡C-R)) character. By incorporating different alkynyl ligands into the periphery of these branched complexes, one could readily tune the nature of the lowest energy emissive state and the direction of the excitation energy transfer.

Keywords: alkynes · energy transfer · luminescence · P ligands · platinum

Introduction

Excitation energy transfer plays an important role in natural processes.[1,2] Many molecular devices have been designed and constructed to harvest solar energy, and dendrimers are probably one of the very few promising candidates that are designed to mimic the natural photosynthetic process.[3] The construction and luminescence properties of various types of organic dendrimers have been extensively investigated in the past few decades.[4–9] In particular, the luminescence and energy-transfer properties of a series of phenylene dendrimers have been extensively investigated by Moore and coworkers.[10]

With the increasing interest in the unique chemical and physical properties possessed by metal complexes, metal-containing dendritic molecules have also attracted much attention and have been extensively investigated. Some of these molecules have found applications in the field of catalysis[11–13] and sensor technologies.[14–16] Metal-containing dendrimers with metal centers in each generation have been scarce due to a lack of appropriately designed building blocks; however, during the last decade, different synthetic protocols have been developed by various groups towards the synthesis of such materials.[17] For instance, the preparation of organometallic platinum-containing dendrimers with a rigid alkynyl backbone has been accomplished by the groups of Stang and Takahashi.[18,19] There were also reports by the groups of Schanze and Lewis on the luminescence properties of organoplatinum(II) alkynyl complexes, oligomers, and polymers.[20–26]

In view of the increasing interest in metal-containing dendrimers, as well as our on-going effort to study the luminescence properties of transition-metal alkynyl complexes,[27–30]

[a] Dr. C.-H. Tao, Dr. N. Zhu, Prof. Dr. V. W.-W. Yam
Centre for Carbon-Rich Molecular and Nano-Scale Metal-Based Materials Research, and Department of Chemistry
The University of Hong Kong, Pokfulam Road, Hong Kong (P.R. China)
Fax: (+852) 2857-1586
E-mail: wwyam@hku.hk

 DOI: 10.1002/chem.200400888

we have investigated the luminescence properties of a series of branched chloropalladium(II) and chloroplatinum(II) alkynyl complexes, which were found to emit from an intraligand triplet (^{3}IL) excited state at low temperature.[31,32] It is envisaged that the previously synthesized chloroplatinum(II) alkynyl complexes [1,3,5-{Cl(PEt_3)$_2$PtC≡CC_6H_4C≡C}$_3C_6H_3$] (**1**) and [1,3-{Cl(PEt_3)$_2$PtC≡CC_6H_4C≡C}$_2$-5-{(iPr)$_3$SiC≡C}C_6H_3] (**2**) are promising precursors for branched luminescent materials or dendrimers that emit from the ^{3}IL excited states.

As an extension of this work, we have directed our goal towards the study of the luminescence and energy transfer properties of a series of branched platinum(II) alkynyl complexes, [1,3,5-{RC≡C(PEt_3)$_2$PtC≡CC_6H_4C≡C}$_3C_6H_3$] (R = C_6H_5 (**3**), C_6H_4OMe (**4**), C_6H_4Me (**5**), $C_6H_4CF_3$ (**6**), C_5H_4N (**7**), C_6H_4SAc (**8**), 1-napthyl (Np; **9**), 1-pyrenyl (Pyr; **10**), 1-anthryl-8-ethynyl (HC≡CAn; **11**)), [1,3-{PyrC≡C(PEt_3)$_2$PtC≡C-C_6H_4C≡C}$_2$-5-{(iPr)$_3$SiC≡C}C_6H_3] (**12**), and [1,3-{PyrC≡C-(PEt_3)$_2$PtC≡CC_6H_4C≡C}$_2$-5-(HC≡C)C_6H_3] (**13**; Scheme 1). With judicious design and choice from a wide variety of alkynyl ligands, the luminescence and electrochemical properties, as well as the direction of energy transfer of the complexes, could be readily tuned and modified. Herein are reported the synthesis, structural characterization, lumines-

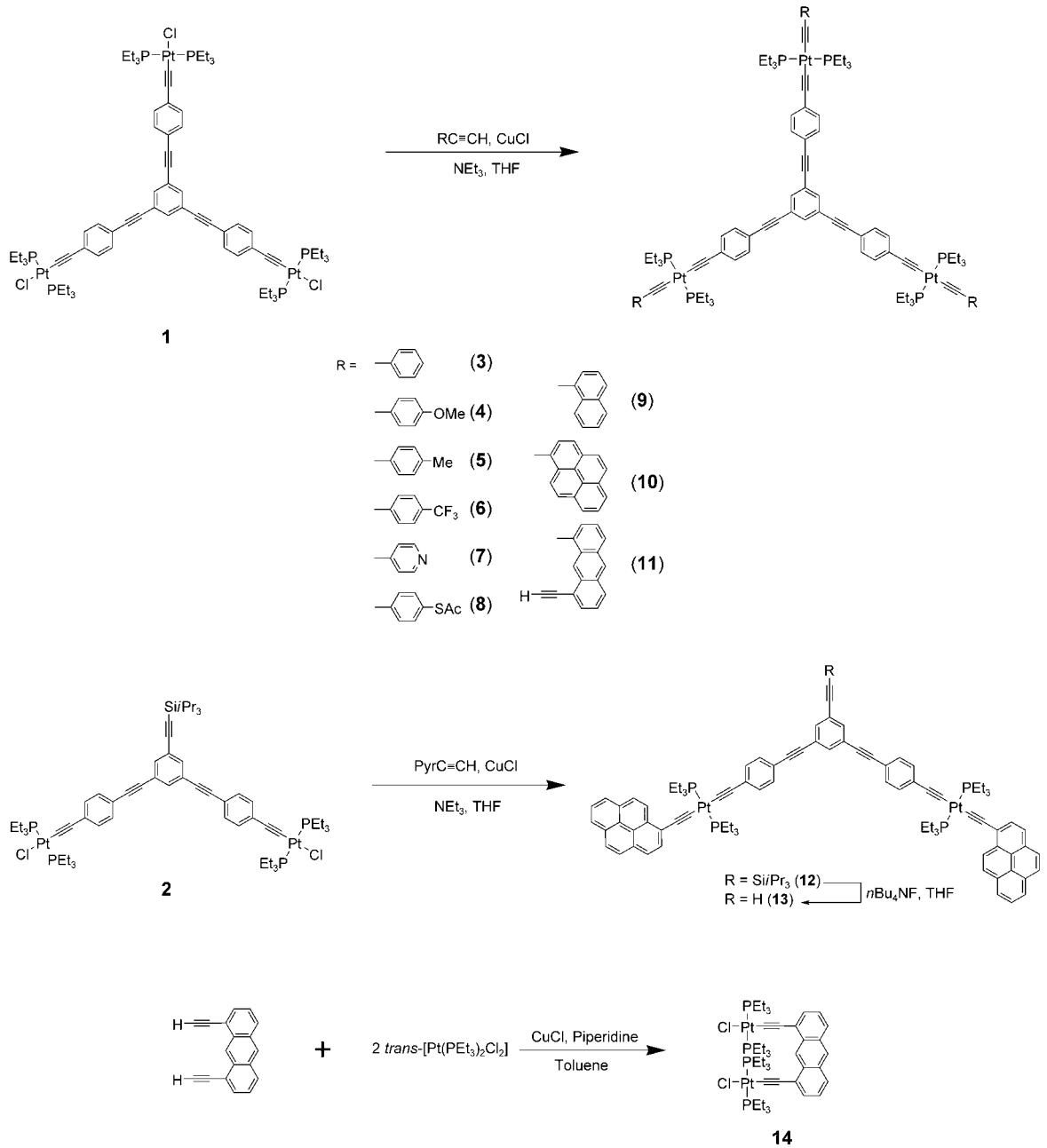

Scheme 1. Syntheses of multinuclear carbon-rich platinum(II) complexes of branched alkynyls. THF = tetrahydrofuran.

cence properties, and electrochemical behavior of a series of luminescent multinuclear platinum(II) complexes of branched rigid alkynyls.

Results and Discussion

Synthesis and characterization: The branched dinuclear chloroplatinum(II) complex **2** was obtained by modification of the preparation of the related trinuclear complex **1** which was reported previously (Scheme 1).[32] To depolymerize the oligomeric materials during the course of the reaction, the complex was prepared in refluxing toluene and piperidine in the presence of a catalytic amount of CuCl. The branched platinum(II) alkynyl complexes **3**–**12** were synthesized by using a copper(I)-catalyzed dehydrohalogenation approach with the multinuclear precursor complexes **1** or **2** as the strating materials. Complexes **3**–**12** were obtained in reasonable yields with various alkynes, thereby demonstrating that the branched multinuclear chloroplatinum(II) complexes **1** and **2** are versatile and promising starting materials for the synthesis of luminescent carbon-rich metal-containing materials.

In the synthesis of complex **8**, ethyldiisopropylamine was used instead of diethylamine. The use of a more sterically hindered amine was essential in the preparation of the sulfur-containing platinum or palladium alkynyl complexes. In particular, the use of ethyldiisopropylamine is crucial in the preparation of the 4-trimethylsilylethynylbenzenethioacetate from the 4-iodobenzenethioacetate through a palladium(II)-catalyzed Sonogashira coupling reaction.[33–35]

In addition, attempts have also been made to synthesize multinuclear complexes with 1,8-diethynylanthracenyl moieties. A trinuclear platinum alkynyl complex, **11**, was isolated in good yield by using complex **1** as the precursor, while a dinuclear chloroplatinum(II) complex [1,8-{$Cl(PEt_3)_2PtC{\equiv}C$}$_2$-An] (**14**) was also isolated by using a synthetic strategy similar to that of complexes **1** and **2** by refluxing 1,8-diethynylanthracene with an excess of *trans*-[$Pt(PEt_3)_2Cl_2$] in the presence of a catalytic amount of CuCl. With the versatility demonstrated by the chloroplatinum(II) alkynyl complexes **1** and **2**, the "metallo-clip" **14** is a potential building block for the construction of multinuclear platinum-containing assemblies.

All the complexes gave satisfactory elemental analyses and have been characterized by IR, ^{1}H NMR, and ^{31}P{^{1}H} NMR spectroscopy and FAB mass spectrometry. The X-ray crystal structures of complexes **4** and **14** have also been determined.

The ^{31}P NMR spectra of all the branched complexes **3**–**13** show a singlet in the range of $\delta = 11.10$–12.05 ppm, which is indicative of the highly symmetrical structure of the complexes. Platinum satellites with $J_{Pt,P}$ values of approximately 2350 Hz were observed, which are indicative of a *trans*-P–Pt–P configuration about the platinum metal centers.

Crystal structure determination: Figures 1 and 2 depict the perspective drawings of complexes **4** and **14**, respectively, and selected bond lengths and angles for both complexes are given in Table 1. All the platinum atoms in complexes **4** and **14** were found to adopt a slightly distorted *trans*-square-planar geometry with the P-Pt-C and P-Pt-Cl angles in the range of 86.2(3) and 92.8(3)°. It is conceivable that such distortion around the coordination plane could be a result of the steric demand of the bulky triethylphosphine ligands. The C≡C bond lengths in both complexes lie in the range of 1.159–1.270 Å, values that are comparable to those found in other mononuclear platinum(II) σ-alkynyl complexes.[18,19,36] The Pt–C bond lengths in **4** (2.001(10)–2.045(10) Å) are considerably longer than that found in **14** (1.865(12) Å), a fact ascribed to the stronger *trans* influence of the alkynyl group compared to that of the chloro group.

The coordination planes about the platinum atoms are not coplanar with the aromatic rings and give interplanar angles of 18.6–89.8° in **4** and 57.4° in **14**; this is a characteristic feature observed for platinum σ-aryl-alkynyl complexes.[18,19,36] The separation between the two platinum

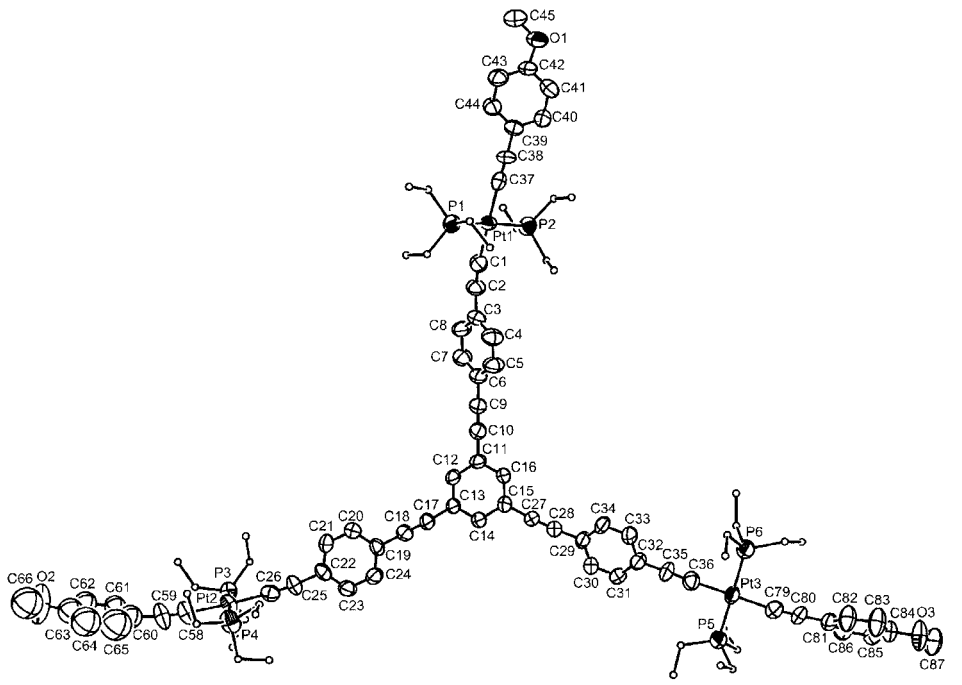

Figure 1. Perspective view of **4** with atomic numbering scheme. Hydrogen atoms have been omitted for clarity. Thermal ellipsoids are shown at 50% probability level. See Table 1 for selected bond lengths and angles.

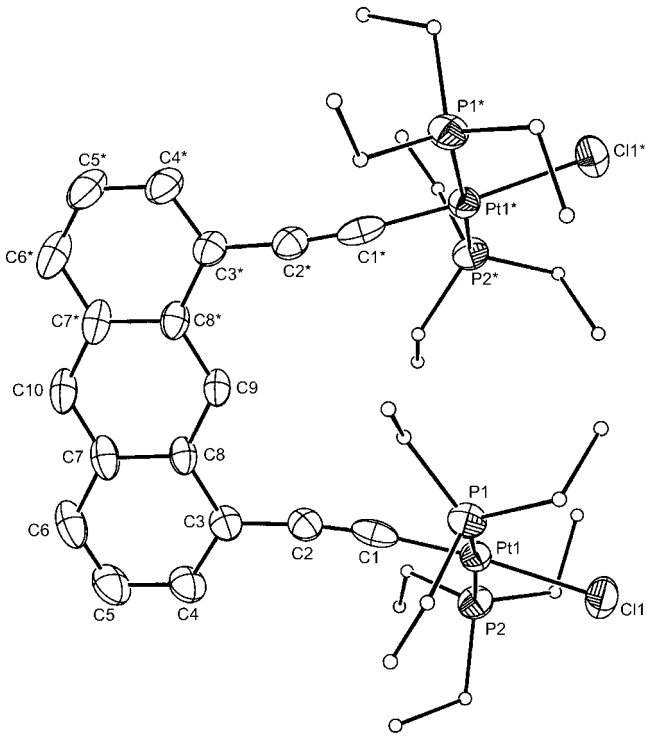

Figure 2. Perspective view of **14** with atomic numbering scheme. Hydrogen atoms have been omitted for clarity. Thermal ellipsoids are shown at 30% probability level. See Table 1 for selected bond lengths and angles.

Table 1. Selected bond lengths [Å] and bond angles [°] for **4** and **14** with estimated standard deviations in parentheses.

Complex			
	Complex **4**		
Pt1−C1	2.016(10)	C17−C18	1.193(12)
Pt1−C37	2.045(10)	C25−C26	1.181(11)
Pt2−C26	2.001(10)	C27−C28	1.178(11)
Pt2−C58	2.005(11)	C35−C36	1.200(11)
Pt3−C36	2.006(9)	C37−C38	1.191(11)
Pt3−C79	2.042(9)	C58−C59	1.159(13)
C1−C2	1.173(11)	C79−C80	1.183(11)
C9−C10	1.186(12)		
C1-Pt1–P2	86.2(3)	C27-C28-C29	176.0(10)
C37-Pt1-P2	91.9(2)	C18-C17-C13	175.5(10)
C1-Pt1-P1	91.9(3)	C17-C18-C19	179.1(11)
C37-Pt1-P1	90.1(2)	C36-C35-C32	176.1(11)
C2-C1-Pt1	175.2(10)	C35-C36-Pt3	178.4(9)
C1-C2-C3	173.5(9)	C38-C37-Pt1	176.5(8)
C10-C9-C6	170.1(11)	C37-C38-C39	176.2(10)
C9-C10-C11	174.4(11)	C59-C58-Pt2	174.1(12)
C26-C25-C22	177.6(11)	C58-C59-C60	173.1(15)
C25-C26-Pt2	173.5(11)	C80-C79-Pt3	173.2(9)
C28-C27-C15	175.9(9)	C79-C80-C81	179.1(12)
	Complex **14**		
Pt1−C1	1.865(12)	Pt1−Cl1	2.364(3)
Pt1−P1	2.304(3)	C1−C2	1.270(14)
Pt1−P2	2.309(3)		
C1-Pt1-P1	86.5(2)	P2-Pt1-Cl1	88.69(9)
C1-Pt1-P2	91.4(2)	C2-C1-Pt1	173.5(8)
P1-Pt1-Cl1	92.74(9)	C1-C2-C3	173.7(10)

atoms in **14** is approximately 6.37 Å, which exceeds the distance for the existence of any Pt···Pt interaction. In fact, the two platinum atoms are bending away from each other, as evidenced by the C2-C1-Pt and C1-C2-C3 bond angles which smaller than the expected 180° for a sp-hybridized carbon atom.

Electronic absorption and emission: The electronic absorption spectra of the branched platinum(II) alkynyl complexes **2–8** show absorption bands in the range of 258–340 nm and 360–368 nm with extinction coefficients of the order of 10^4–10^5 $dm^3 mol^{-1} cm^{-1}$ (Figure 3). Table 2 summarizes the photophysical data of the complexes. With reference to previous spectroscopic works on *trans*-$[Pt(PEt_3)_2(C{\equiv}CR)_2]$,[37–41] in which the absorption bands at approximately 300–360 nm were assigned as metal-to-alkynyl metal-to-ligand charge transfer (MLCT) transitions, it is likely that the low-energy transitions in these branched complexes would also involve a certain degree of MLCT character. Another piece of evidence for a MLCT assignment of the low-energy absorption bands in these complexes was provided by the resonance Raman investigation of *trans*-$[Pt(PEt_3)_2(C{\equiv}CH)_2]$ and *trans*-$[Pt(dppm)_2(C{\equiv}CPh)_2]$ (dppm = 1,2-bis(diphenylphosphino)-methane).[38,41] It was demonstrated that the initial excited-state vibrational reorganizational energy and displacement were mostly along the nominal C≡C stretch; this is in line with an assignment of the absorption band to a MLCT (Pt→C≡CR) transition.[37–41] In addition, the lengthening of the C≡C bond in the initial ^{1}MLCT excited states of the

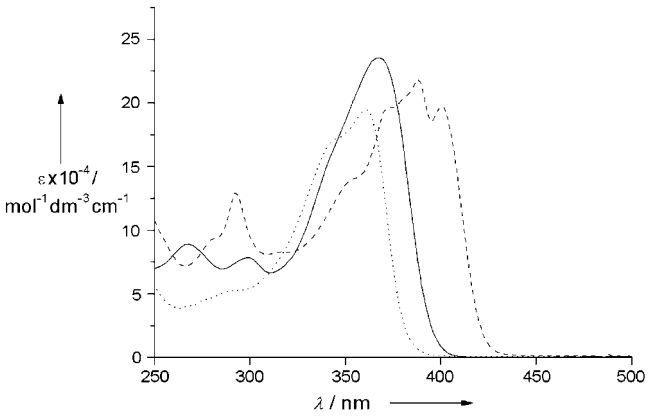

Figure 3. Electronic absorption spectra of **1** (•••••), **3** (——), and **10** (-----) in dichloromethane at room temperature.

mononuclear complexes relative to their ground states was found to be consistent with an expected nominal bond-order change from 3 to 2.5 for a Pt→π*(C≡CR) metal-to-ligand charge transfer.[37–41] However, the very slight to almost no influence on the absorption energies of the branched complexes **3–8** that is exerted by the peripheral aryl-alkynyl ligands would suggest that the absorption pattern is dominated by intraligand (π→π*(C≡CR)) transitions. Thus, the absorptions in these branched complexes are best described as an admixture of IL (π→π*(C≡CR)) and MLCT (dπ(Pt)→π*(C≡CR)) transitions with predominantly IL character. It is noteworthy that a slight red shift in absorption energy of

Table 2. Electronic absorption and photophysical data for complexes **2**–**14**.

Complex	λ [nm] (ε [$dm^3 mol^{-1} cm^{-1}$])[a]	Medium (T [K])	λ_{em} [nm] (τ_o [μs])
2	258 (46210), 270 sh (43370), 340 (92540), 360 (104080)	CH_2Cl_2 (298)	531 (6.5)
		solid (298)	527 (6.0)
		solid (77)	527 (74.7)
		glass (77)[b]	532 (350)
3	268 (78850), 298 (72470), 338 sh (141600), 366 (228900)	CH_2Cl_2 (298)	532 (49.7)
		solid (298)	533 (0.2)
		solid (77)	538 (74.5)
		glass (77)[b]	533 (359)
4	268 (88870), 298 (78380), 338 sh (140530), 368 (235480)	CH_2Cl_2 (298)	535 (45.6)
		solid (298)	532 (7.1)
		solid (77)	530 (127)
		glass (77)[b]	530 (394)
5	268 (79610), 298 (71610), 338 sh (134590), 364 (213650)	CH_2Cl_2 (298)	532 (41.4)
		solid (298)	530 (0.15)
		solid (77)	538 (115)
		glass (77)[b]	528 (409)
6	274 (55640), 298 (59180), 338 sh (121900), 366 (195090)	CH_2Cl_2 (298)	532 (60.8)
		solid (298)	533 (0.14)
		solid (77)	537 (30.9)
		glass (77)[b]	532 (381)
7	278 (70370), 298 (74960), 364 (210715)	CH_2Cl_2 (298)	531 (47.9)
		solid (298)	532 (0.18)
		solid (77)	536 (29.8)
		glass (77)[b]	532 (371)
8	280 (61605), 300 (75520), 366 (169270)	CH_2Cl_2 (298)	532 (49.8)
		solid (298)	533 (0.16)
		solid (77)	534 (30.1)
		glass (77)[b]	532 (412)
9	308 (78380), 370 (244950)	CH_2Cl_2 (298)	546 (60.8)
		solid (298)	–[c]
		solid (77)	548 (13.4)
		glass (77)[b]	543 (438)
10	280 (92765), 292 (129200), 352 sh (138440), 372 sh (196190), 388 (218465), 400 (197640)	CH_2Cl_2 (298)	660 (45.2)
		solid (298)	–[c]
		solid (77)	–[c]
		glass (77)[b]	655 (244)
11	256 (251010), 270 sh (181495), 278 sh (154015), 302 sh (74025), 342 sh (146190), 364 (174590), 404 (60145), 428 (53460)	CH_2Cl_2 (298)	744 (37.2)
		solid (298)	–[c]
		solid (77)	–[c]
		glass (77)[b]	735 (96.5)
12	276 (64060), 292 (83070), 352 sh (89870), 372 (123310), 388 (133860), 400 (121170)	CH_2Cl_2 (298)	657 (42.8)
		solid (298)	–[c]
		solid (77)	–[c]
		glass (77)[b]	655 (248)
13	276 (94860), 329 (123020), 352 sh (133090), 372 (182615), 388 (198230), 400 (179440)	CH_2Cl_2 (298)	658 (36.1)
		solid (298)	523 (<0.1)
		solid (77)	522 (<0.1)
		glass (77)[b]	655 (218)
14	272 (127440), 354 (7000), 370 (9520), 390 (14080), 410 (24990), 434 (26010)	CH_2Cl_2 (298)	743 (0.2)
		solid (298)	–[c]
		solid (77)	–[c]
		glass (77)[b]	733 (6.8)

[a] Measured in CH_2Cl_2 at 298 K. [b] Measured in a EtOH/MeOH (4:1, v/v) glass. [c] Nonemissive.

the low-energy band is observed on going from the precursor **1** (362 nm) to complexes **3**–**8** (364–368 nm); this result is supportive of a mixing of MLCT (dπ(Pt)→π*(C≡CR)) character and may indicate the presence of conjugation through the metal centers. Similar findings have also been reported in related linear oligomers.[20]

The branched complexes with peripheral polyaromatic alkynyl ligands, **9**–**14**, show highly structured absorption bands at approximately 276–352 nm and 370–434 nm with extinction coefficients of the order of 10^4–10^5 $dm^3 mol^{-1} cm^{-1}$. In view of the similar absorption patterns and extinction coefficients with their corresponding free polyaromatic alkynes, the assignment of IL (π→π*(C≡CR)) transitions is favored, although the possibility of an involvement of a MLCT (dπ(Pt)→π*(C≡CR)) transition is also likely for the reasons described above. Again, the transitions in complexes **9**–**14** are similarly assigned as an admixture of IL (π→π*(C≡CR)) and MLCT (dπ(Pt)→π*(C≡CR)) transitions with predominantly IL character.

Upon photoexcitation, all the branched complexes display luminescence in deaerated dichloromethane solutions at room temperature (Figure 4). All complexes show lifetimes

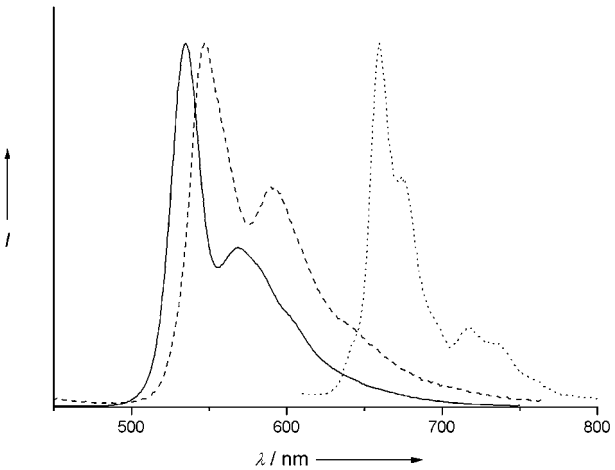

Figure 4. Emission spectra of **3** (——), **9** (-----), and **10** (•••••) in dichloromethane at room temperature.

in the microsecond range, which is indicative of their triplet parentage. The strong spin-orbit coupling introduced by the heavy platinum(II) metal center enhances the accessibility of the ^{3}IL (π→π*) excited states and renders the $Pt(PEt_3)_2$ moiety a good building unit to access the spin-forbidden ^{3}IL excited states. In contrast to the nonemissive behavior of the precursor complex **1** at room temperature, complexes **3**–**8** show intense yellowish green luminescence at about 531–535 nm, with vibrational progressional spacings of approximately 1130 and 2160 cm^{-1} in both the solution and solid-state emission spectra at room temperature. It is interesting to note that complexes **3**–**8** emit at nearly identical wavelengths with similar vibronic structures to the chloroplatinum(II) precursor complex **1** both in the solid state and in an alcoholic glass at 77 K. The emission energies of these complexes appear to be insensitive to the electron-withdrawing or -donating nature of the substituents on the peripheral aryl-alkynyl ligands. These findings are supportive of a triplet emission emanating mainly from the central $(C{\equiv}C\text{-}C_6H_4C{\equiv}C)_3C_6H_3$ moiety. However, a red shift in the emis-

sion energies is observed for the branched complexes on going from the palladium complexes to the platinum analogues; this is indicative of the involvement of triplet metal-to-alkynyl MLCT character in the emissive states.[32] In addition, a recent theoretical study on related mononuclear platinum(II) alkynyl complexes, *trans*-$[Pt(PEt_3)_2(C{\equiv}CPh)_2]$ and *trans*-$[Pt(PEt_3)_2(C{\equiv}CC_6H_4C{\equiv}CH)_2]$, by Brozik and co-workers using density functional theory[42] showed that a d orbital on the platinum atom is directly involved in the π system in the highest occupied molecular orbital (HOMO) of the complexes they studied. The lowest unoccupied molecular orbital (LUMO) of the complexes, on the other hand, has essentially no electron density located on the platinum metal, a result that is in line with an emission from a mixed ^{3}IL ($\pi\rightarrow\pi^*(C{\equiv}CR)$]/^{3}MLCT ($d\pi(Pt)\rightarrow\pi^*(C{\equiv}CR)$) manifold. It is interesting to note that emission from the ^{3}IL state of the peripheral alkynyl ligands was not observed in these complexes owing to their relatively high-lying energy, and the energy absorbed by the peripheral ligands would probably be transferred to the central emitting core (Figure 5).

Degassed dichloromethane solutions of the branched platinum(II) alkynyl complexes with polyaromatic peripheral ligands **9**–**14** show emission in the yellow to red region with lifetimes in the microsecond range. Shorter lifetimes were observed for complexes **11** and **14**, which emit at relatively lower energies, in line with the energy-gap law. Vibrational progressional spacings of approximately 1360–1380 cm^{-1} were observed in the emission spectra of complexes **9**–**13**, which is typical of the C=C stretching mode of the aromatic rings. With reference to previous work on *cis*-[Pt(dppe)(C≡C-Np)$_2$] (dppe = 1,2-bis(diphenylphosphino)ethane)[43] and *trans*-$[Pt(PnBu_3)_2(C{\equiv}CPyr)_2]$,[44] in which the ^{3}IL emissions of these platinum complexes with polyaromatic alkynyl ligands also occur at similar energies with comparable vibronic structures, these highly structured emissions of complexes **9**–**11** are likely to be of mainly ^{3}IL character. However, the involvement of MLCT character could not be completely ruled out; thus, the emissions of complexes **9**–**11** are tentatively assigned as being derived from a mixed ^{3}IL ($\pi\rightarrow\pi^*(C{\equiv}CR)$)/^{3}MLCT ($d\pi(Pt)\rightarrow\pi^*(C{\equiv}CR)$) state with predominantly IL character. It is noteworthy that the ^{3}IL emission from the central $(C{\equiv}CC_6H_4C{\equiv}C)_3C_6H_3$ moieties could not be observed, probably due to the existence of another lower lying ^{3}IL excited state upon coordination of the polyaromatic alkynyl ligands, in which case the energy absorbed by the central core would be transferred to the lowest energy emissive state of the peripheral ligands (Figure 5). By incorporating different alkynyl ligands into the periphery of these branched complexes, one could control the direction of energy transfer; this work represents a rational design and synthesis of branched platinum(II) alkynyl complexes with desired directional energy transfer.

Electrochemical properties: The cyclic voltammograms of the platinum(II) alkynyl complexes **1**–**14** do not show observable reduction waves upon scanning up to −2.0 V (all values measured versus the saturated calomel electrode (SCE)), while the oxidative scans of complexes **1**–**14** generally show two or three irreversible oxidation waves at +0.86 to +1.27, +1.33 to +1.74, and +1.87 to +1.98 V. Table 3 summarizes the electrochemical data of the branched platinum(II) alkynyl complexes.

Table 3. Electrochemical data for complexes **1**–**14**[a].

Complex	Oxidation E_{pa} [V versus the SCE][b]
1	+1.27
2	+1.25, +1.59, +1.87
3	+1.12, +1.64
4	+0.99, +1.65
5	+1.12, +1.64
6	+1.20, +1.68
7	+1.21, +1.69
8	+1.20, +1.68
9	+1.07, +1.88
10	+0.93, +1.72, +1.98
11	+0.98, +1.60
12	+0.93, +1.74
13	+0.92, +1.73
14	+0.86, +1.33

[a] In dichloromethane (0.1 M nBu_4NPF_6); working electrode, glassy carbon; scan rate = 100 $mV\,s^{-1}$. [b] E_{pa} refers to the anodic peak potential for the irreversible oxidation waves.

The first oxidation waves observed for complexes **3**–**8** (+0.99 to +1.20 V) were found to occur at potentials similar to those of their chloroplatinum(II) precursor complexes **1** and **2**, in which potentials of +1.27 and +1.25 V were ob-

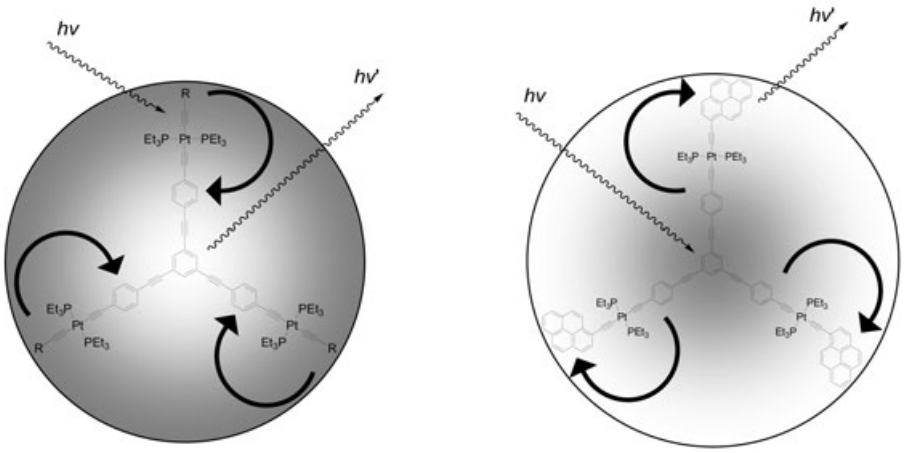

Figure 5. Representation of energy transfer in multinuclear carbon-rich platinum(II) complexes of branched alkynyls.

served for their first oxidations, respectively. Slightly less positive potentials were observed for complexes **3–8** compared to their precursors and this observation is in line with the slight red shifts observed in the lowest energy absorption and emission bands in their respective electronic absorption and emission spectra. Given the first oxidation of R–$C_6H_4C{\equiv}CH$ occurred at approximately +1.5 to + 1.7 V,[45] which is a more positive potential than the conjugated alkynes $(HC{\equiv}CC_6H_4C{\equiv}C)_3C_6H_3$ (about +1.35 V), the first oxidation waves of complexes **3–8** are probably due to the oxidation of the central organic $(C{\equiv}CC_6H_4C{\equiv}C)_3C_6H_3$ backbone. However, the less positive potentials for the first oxidation waves observed for the platinum complexes **1** (+1.27 V) and **2** (+1.25 V), compared to those of their palladium analogues, $[1,3,5\text{-}\{Cl(PEt_3)_2PdC{\equiv}CC_6H_4C{\equiv}C\}_3C_6H_3]$ (+1.34 V) and $[1,3\text{-}\{Cl(PEt_3)_2PdC{\equiv}CC_6H_4C{\equiv}C\}_2\text{-}5\text{-}\{(i\text{Pr})_3SiC{\equiv}C\}C_6H_3]$ (+1.38 V), are indicative of the presence of some metal character in their HOMO; this is in line with the red shift in the absorption and emission energies on going from the palladium complexes to the platinum complexes. It is likely that the two irreversible oxidation waves for this class of complex may also possess a certain degree of metal-centered character; thus the two irreversible oxidation waves of complexes **3–8** could be best described as ligand-centered oxidation with some mixing of metal-centered character.

For the platinum(II) alkynyl complexes with polyaromatic ligands **9–14**, the first oxidation waves were found in the range of +0.86 to +1.07 V, values that are slightly less positive than those of **3–8** (+0.99 to +1.20 V) and their chloroplatinum(II) precursor complexes **1** (+1.27 V) and **2** (+1.25 V). The large shift in the potential for the first oxidation of **14** (+0.86 V) relative to that of the branched chloroplatinum(II) complex **1** (+1.27 V) is indicative of an oxidation that is predominantly ligand-centered in character. This, together with the less positive potentials for the oxidation of the polyaromatic alkynes (+1.0 to +1.2 V)[46] relative to that of $1,3,5\text{-}(HC{\equiv}CC_6H_4C{\equiv}C)_3C_6H_3$ (approximately +1.35 V), suggested that the first oxidation waves of complexes **9–14** are probably derived from the ligand-centered oxidation of the polyaromatic alkynyl ligands. However, an involvement of some metal-centered character could not be completely ruled out. The predominantly ligand-centered origin of these first oxidations observed for complexes **1–14** agrees well with the assignment of a predominantly ligand-centered character for both the electronic absorption and emission behavior of these complexes.

Conclusion

A series of luminescent platinum(II) alkynyl complexes, $[1,3,5\text{-}\{RC{\equiv}C(PEt_3)_2PtC{\equiv}CC_6H_4C{\equiv}C\}_3C_6H_3]$ where R = C_6H_5, C_6H_4OMe, C_6H_4Me, $C_6H_4CF_3$, C_5H_4N, C_6H_4SAc, Np, Pyr or HC≡CAn, $[1,3\text{-}\{PyrC{\equiv}C(PEt_3)_2PtC{\equiv}CC_6H_4C{\equiv}C\}_2\text{-}5\text{-}\{(i\text{Pr})_3SiC{\equiv}C\}C_6H_3]$, $[1,3\text{-}\{PyrC{\equiv}C(PEt_3)_2PtC{\equiv}CC_6H_4C{\equiv}C\}_2\text{-}5\text{-}(HC{\equiv}C)C_6H_3]$, and $[1,8\text{-}\{Cl(PEt_3)_2PtC{\equiv}C\}_2An]$ were successfully synthesized. The crystal structures of $[1,3,5\text{-}\{MeOC_6H_4C{\equiv}C(PEt_3)_2PtC{\equiv}CC_6H_4C{\equiv}C\}_3C_6H_3]$ and $[1,8\text{-}\{ClPt(PEt_3)_2C{\equiv}C\}_2An]$ were determined, thereby confirming the distorted square planar geometry at the platinum center, with bond lengths in the normal ranges expected for this class of compounds. These complexes are found to be emissive at room temperature with rich vibronic structures; their lowest lying emissive states were tunable and assigned to be derived from predominantly ^{3}IL states, either of the central $(C{\equiv}CC_6H_4C{\equiv}C)_3C_6H_3$ moiety or the peripheral polyaromatic alkynyl ligands, probably mixed with some ^{3}MLCT ($d\pi(Pt)\rightarrow\pi^*(C{\equiv}CR)$) character. Through rational design and synthetic methodologies, the direction of energy transfer in branched platinum(II) alkynyl complexes can be easily tuned.

Experimental Section

Materials and reagents: $[1,3,5\text{-}\{Cl(PEt_3)_2PtC{\equiv}CC_6H_4C{\equiv}C\}_3C_6H_3]$ (**1**),[32] $1,3\text{-}\{HC{\equiv}CC_6H_4C{\equiv}C\}_2\text{-}5\text{-}\{(i\text{Pr})_3SiC{\equiv}C\}C_6H_3$,[47] 4-ethynylpyridine,[48] 4-ethynylbenzenethioacetate,[49] and 1,8-diethynylanthracene[50] were synthesized according to literature procedures. Ethynylbenzene (Aldrich, 98%), 1-ethynyl-4-methoxybenzene (Maybridge), 1-ethynyltoluene (GFS, 98%), 1-ethynyl-4-trifluoromethylbenzene (Aldrich, 97%), 1-ethynylnaphthalene (Aldrich, 97%), 1-ethynylpyrene (Lancaster, 96%), and $n\text{Bu}_4\text{NF}$ (1 M solution in THF; Lancaster) were purchased and used as received. All organic amines were distilled over potassium hydroxide and stored over potassium hydroxide prior to use. All other solvents and reagents were of analytical grade and used as received.

Syntheses:

$[1,3\text{-}\{Cl(PEt_3)_2PtC{\equiv}CC_6H_4C{\equiv}C\}_2\text{-}5\text{-}\{(i\text{Pr})_3SiC{\equiv}C\}C_6H_3]$ (2): This was synthesized according to a modified version of a literature procedure for the synthesis of complex **1**.[32] *trans*-$[Pt(PEt_3)_2Cl_2]$ (1.000 g, 1.99 mmol) and $1,3\text{-}(HC{\equiv}CC_6H_4C{\equiv}C)_2\text{-}5\text{-}\{(i\text{Pr})_3SiC{\equiv}C\}C_6H_3$ (252 mg, 0.50 mmol) were dissolved in a mixture of toluene (70 mL) and piperidine (5 mL). The reaction mixture was heated to reflux for 30 min after which CuCl (5 mg, 0.04 mmol) was added and the reaction mixture was then refluxed under nitrogen for two days. The solvent was removed under vacuum and the yellow oily residue was dissolved in dichloromethane and washed successively with aqueous ammonium chloride solution and deionized water. The organic fraction was then dried over anhydrous $MgSO_4$ and filtered. Purification was accomplished by column chromatography (basic aluminum oxide, 50–200 microns), in which the excess *trans*-$[Pt(PEt_3)_2Cl_2]$ was first eluted with dichloromethane/petroleum ether (1:1, v/v) and then **2** was eluted with dichloromethane. Subsequent recrystallization from benzene/*n*-pentane afforded **2** as a very pale yellow microcrystalline solid: Yield = 504 mg, 70%; ^{1}H NMR (400 MHz, $CDCl_3$, 298 K, relative to Me_4Si): $\delta = 1.14$ (s, 21H; *i*Pr), 1.21 (vq, $J = 5.0$ Hz, 36H; CH_3), 2.03–2.12 (m, 24H; CH_2–P), 7.22 (d, 4H, $J(H,H) = 11.0$ Hz; C_6H_4), 7.36 (d, 4H, $J(H,H) = 11.0$ Hz; C_6H_4), 7.55 (d, 2H, $J(H,H) = 1.5$ Hz; C_6H_3), 7.59 ppm (s, 1H, $J(H,H) = 1.5$ Hz; C_6H_3); ^{13}C{^{1}H} NMR (125.8 MHz, $CDCl_3$, 298 K, relative to Me_4Si): $\delta = 8.04$ (s; CH_3), 11.29 (s; *i*Pr), 14.56 (t, $J(C,P) = 17.0$ Hz; CH_2–P), 18.67 (s; *i*Pr), 86.46 (t, $J_{C,P} = 16.0$ Hz; acetylenic carbons), 88.48, 90.99, 92.08, 101.85, 105.38 (s; acetylenic carbons), 119.21, 124.09, 124.17, 129.18, 130.82, 131.36, 133.89, 134.16 ppm (s; aromatic carbons); ^{31}P{^{1}H} NMR (162 MHz, $CDCl_3$, 298 K, relative to 85% H_3PO_4): $\delta = 15.30$ (s, $J(Pt,P) = 2381$ Hz) ppm; IR (KBr disc): $\tilde{\nu} = 2114$(s), 2154(w), 2211(w) cm^{-1}, $\tilde{\nu}$(C≡C); positive-ion FAB MS: *m/z*: 1439 $[M]^+$; elemental analysis calcd (%) for **2**: C 50.9, H 6.45; found: C 50.7, H 6.28.

$[1,3,5\text{-}\{C_6H_5C{\equiv}C(PEt_3)_2PtC{\equiv}CC_6H_4C{\equiv}C\}_3C_6H_3]$ (3): This was synthesized according to a modified version of a literature procedure for the synthesis of related compounds.[19] Complex **1** (142 mg, 0.077 mmol) and ethynylbenzene (26 mg, 0.252 mmol) were dissolved in a mixture of THF

(20 mL) and diethylamine (10 mL). CuCl (5 mg) was added to this reaction mixture as a catalyst. The pale-yellow mixture was then stirred overnight at room temperature, and the solvent was removed under reduced pressure. The greenish-yellow gummy residue was then redissolved in dichloromethane, washed successively with brine and deionized water, and dried over anhydrous sodium sulfate. The solution was then filtered, and the solvent was removed under reduced pressure. The yellow residue was chromatographed on basic aluminum oxide (50–200 microns) with dichloromethane as the eluent. Subsequent recrystallization of the crude product with dichloromethane/*n*-hexane afforded **3** as a pale-yellow powder: Yield = 68 mg, 43%; ^{1}H NMR (400 MHz, $CDCl_3$, 298 K, relative to Me_4Si): $\delta = 1.22$ (vq, $J = 8.0$ Hz, 54H; CH_3), 2.10–2.20 (m, 36H; CH_2–P), 7.10–7.30 (m, 21H; C_6H_5 and C_6H_4), 7.36 (d, 6H, J(H,H) = 8.2 Hz; C_6H_4), 7.60 ppm (s, 3H; C_6H_3); ^{31}P{^{1}H} NMR (162 MHz, $CDCl_3$, 298 K, relative to 85% H_3PO_4): $\delta = 11.18$ ppm (s, J(Pt,P) = 2366 Hz); IR (KBr disc): $\tilde{\nu} = 2099$(s), 2205(w) cm^{-1}, ν(C≡C); positive ion FAB MS: m/z: 2044 $[M+1]^+$; elemental analysis calcd (%) for **3**: C 56.38, H 5.91; found: C 56.52, H 6.01.

[1,3,5-{MeOC$_6$H$_4$C≡C(PEt$_3$)$_2$PtC≡CC$_6$H$_4$C≡C}$_3$C$_6$H$_3$] (4): The procedure was similar to that for **3** except that 1-ethynyl-4-methoxybenzene (33 mg, 0.252 mmol) was used instead of ethynylbenzene to afford **4** as a pale-yellow powder: Yield = 85 mg, 52%; ^{1}H NMR (400 MHz, $CDCl_3$, 298 K, relative to Me_4Si): $\delta = 1.23$ (vq, $J = 8.0$ Hz, 54H; CH_2–CH_3), 2.10–2.25 (m, 36H; CH_2–P), 3.85 (s, 9H; OMe), 6.77 (d, 6H, J(H,H) = 9.0 Hz; C_6H_4OMe), 7.21 (d, 6H, J(H,H) = 9.0 Hz; C_6H_4OMe), 7.24 (d, 6H, J(H,H) = 9.0 Hz; C_6H_4), 7.36 (d, 6H, J(H,H) = 9.0 Hz; C_6H_4), 7.59 ppm (s, 3H; C_6H_3); ^{31}P{^{1}H} NMR (162 MHz, $CDCl_3$, 298 K, relative to 85% H_3PO_4): $\delta = 11.10$ ppm (s, J(Pt,P) = 2374 Hz); IR (KBr disc): $\tilde{\nu} = 2097$(s), 2207(w) cm^{-1}, ν̃(C≡C); positive-ion FAB MS: m/z: 2134 $[M+1]^+$; elemental analysis calcd (%) for **4**: C 55.69, H 5.95; found: C 55.74, H 5.72.

[1,3,5-{MeC$_6$H$_4$C≡C(PEt$_3$)$_2$PtC≡CC$_6$H$_4$C≡C}$_3$C$_6$H$_3$] (5): The procedure was similar to that for **3** except that 1-ethynyltoluene (29 mg, 0.252 mmol) was used instead of ethynylbenzene to afford **5** as pale-yellow powder: Yield = 80 mg, 50%; ^{1}H NMR (400 MHz, $CDCl_3$, 298 K, relative to Me_4Si): $\delta = 1.22$ (vq, $J = 8.0$ Hz, 54H; CH_2–CH_3), 2.10–2.25 (m, 36H; CH_2–P), 2.29 (s, 9H; C_6H_4*Me*), 7.01 (d, 6H, J(H,H) = 8.0 Hz; C_6H_4Me), 7.18 (d, 6H, J(H,H) = 8.0 Hz; C_6H_4Me), 7.24 (d, 6H, J(H,H) = 12.0 Hz; C_6H_4), 7.30 (d, 6H, J(H,H) = 12.0 Hz; C_6H_4), 7.60 ppm (s, 3H; C_6H_3); ^{31}P{^{1}H} NMR (162 MHz, $CDCl_3$, 298 K, relative to 85% H_3PO_4): $\delta = 11.18$ ppm (s, J(Pt,P) = 2393 Hz); IR (KBr disc): $\tilde{\nu} = 2099$(s), 2207(w) cm^{-1}, ν(C≡C); positive-ion FAB MS: m/z: 2085 $[M]^+$; elemental analysis calcd (%) for **5**: C 56.97, H 6.08; found: C 57.10, H 6.13.

[1,3,5-{F$_3$CC$_6$H$_4$C≡C(PEt$_3$)$_2$PtC≡CC$_6$H$_4$C≡C}$_3$C$_6$H$_3$] (6): The procedure was similar to that for **3** except that 1-ethynyl-4-trifluoromethylbenzene (43 mg, 0.252 mmol) was used instead of ethynylbenzene to afford **6** as a pale-yellow powder: Yield = 81 mg, 47%; ^{1}H NMR (400 MHz, $CDCl_3$, 298 K, relative to Me_4Si): $\delta = 1.23$ (vq, $J = 8.0$ Hz, 54H; CH_3), 2.10–2.20 (m, 36H; CH_2–P), 7.25 (d, 6H, J(H,H) = 8.3 Hz; C_6H_4), 7.34 (d, 6H, J(H,H) = 8.1 Hz; $C_6H_4CF_3$), 7.38 (d, 6H, J(H,H) = 8.3 Hz; C_6H_4), 7.45 (d, 6H, J(H,H) = 8.1 Hz; $C_6H_4CF_3$), 7.60 ppm (s, 3H; C_6H_3); ^{31}P{^{1}H} NMR (162 MHz, $CDCl_3$, 298 K, relative to 85% H_3PO_4): $\delta = 11.33$ ppm (s, J(Pt,P) = 2356 Hz); IR (KBr disc): $\tilde{\nu} = 2100$(s), 2207(w) cm^{-1}, ν(C≡C); positive ion FAB MS: m/z: 2249 $[M+1]^+$; elemental analysis calcd (%) for **6**: C 52.87, H 5.24; found: C 53.04, H 5.37.

[1,3,5-{NC$_5$H$_4$C≡C(PEt$_3$)$_2$PtC≡CC$_6$H$_4$C≡C}$_3$C$_6$H$_3$] (7): The procedure was similar to that described for the preparation of **3** except that 4-ethynylpyridine (26 mg, 0.252 mmol) was used instead of ethynylbenzene to afford **7** as a yellow powder: Yield = 66 mg, 42%; ^{1}H NMR (400 MHz, $CDCl_3$, 298 K, relative to Me_4Si): $\delta = 1.23$ (vq, $J = 8.0$ Hz, 54H; CH_3), 2.20–2.30 (m, 36H; CH_2–P), 7.10 (d, 6H, J(H,H) = 5.4 Hz; C_5H_4N), 7.25 (d, 6H, J(H,H) = 8.2 Hz; C_6H_4), 7.38 (d, 6H, J(H,H) = 8.2 Hz; C_6H_4), 7.61 (s, 3H; C_6H_3), 8.39 ppm (d, 6H, J(H,H) = 5.4 Hz; C_5H_4N); ^{31}P{^{1}H} NMR (162 MHz, $CDCl_3$, 298 K, relative to 85% H_3PO_4): $\delta = 11.35$ ppm (s, J(Pt,P) = 2347 Hz); IR (KBr disc): $\tilde{\nu} = 2095$ (s), 2205(w) cm^{-1}, ν(C≡C); positive-ion FAB MS: m/z: 2048 $[M+1]^+$; elemental analysis calcd (%) for **7**: C 54.54, H 5.76, N 2.05; found: C 54.37, H 5.69, N 2.16.

[1,3,5-{AcSC$_6$H$_4$C≡C(PEt$_3$)$_2$PtC≡CC$_6$H$_4$C≡C}$_3$C$_6$H$_3$] (8): The procedure was similar to that for **3** except that 4-ethynylbenzenethioacetate (44 mg, 0.252 mmol) and ethyldiisopropylamine (10 mL) were used instead of ethynylbenzene and diethylamine, respectively, to afford **8** as a yellow powder: Yield = 50 mg, 29%; ^{1}H NMR (400 MHz, $CDCl_3$, 298 K, relative to Me_4Si): $\delta = 1.22$ (vq, $J = 8.0$ Hz, 54H; CH_2–CH_3), 2.10–2.25 (m, 36H; CH_2–P), 2.40 (s, 9H; SAc), 7.25–7.30 (m, 18H; C_6H_4 and C_6H_4SAc), 7.42 (d, 6H, J(H,H) = 9.0 Hz; C_6H_4), 7.64 ppm (s, 3H; C_6H_3); ^{31}P{^{1}H} NMR (162 MHz, $CDCl_3$, 298 K, relative to 85% H_3PO_4): $\delta = 11.30$ ppm (s, J(Pt,P) = 2360 Hz); IR (KBr disc): $\tilde{\nu} = 2098$(s), 2207(w) cm^{-1}, ν(C≡C); positive-ion FAB MS: m/z: 2266 $[M+1]^+$; elemental analysis calcd (%) for **8**: C 54.03, H 5.60; found: C 54.17, H 5.51.

[1,3,5-{NpC≡C(PEt$_3$)$_2$PtC≡CC$_6$H$_4$C≡C}$_3$C$_6$H$_3$] (9): The procedure was similar to that for **3** except that 1-ethynylnapthalene (38 mg, 0.252 mmol) was used instead of ethynylbenzene to afford **9** as a very pale orange powder: Yield = 106 mg, 63%; ^{1}H NMR (400 MHz, $CDCl_3$, 298 K, relative to Me_4Si): $\delta = 1.22$ (vq, $J = 8.0$ Hz, 54H; CH_3), 2.15–2.25 (m, 36H; CH_2–P), 7.27 (d, 6H, J(H,H) = 8.0 Hz; C_6H_4), 7.34 (d, 3H, J(H,H) = 6.0 Hz; Np), 7.40 (d, 6H, J(H,H) = 8.0 Hz; C_6H_4), 7.42–7.49 (m, 9H; Np), 7.61 (s, 3H; C_6H_3), 7.63 (d, 3H, J(H,H) = 12.0 Hz; Np), 7.80 (d, 3H, J(H,H) = 12.0 Hz; Np), 8.51 ppm (d, 3H, J(H,H) = 12.0 Hz; Np); ^{31}P{^{1}H} NMR (162 MHz, $CDCl_3$, 298 K, relative to 85% H_3PO_4): $\delta = 11.69$ ppm (s, J(Pt,P) = 2365 Hz); IR (KBr disc): $\tilde{\nu} = 2093$(s), 2207(w) cm^{-1}, ν(C≡C); positive-ion FAB MS: m/z: 2194 $[M]^+$; elemental analysis calcd (%) for **9**: C 59.09, H 5.79; found: C 59.21, H 5.62.

[1,3,5-{PyrC≡C(PEt$_3$)$_2$PtC≡CC$_6$H$_4$C≡C}$_3$C$_6$H$_3$] (10): The procedure was similar to that for **3** except that 1-ethynylpyrene (57 mg, 0.252 mmol) was used instead of ethynylbenzene. Subsequent recrystallization of the crude product with dichloromethane/*n*-hexane afforded **10** as a yellow powder: Yield = 114 mg, 61%; ^{1}H NMR (400 MHz, $CDCl_3$, 298 K, relative to Me_4Si): $\delta = 1.30$ (vq, $J = 8.0$ Hz, 54H; CH_3), 2.20–2.30 (m, 36H; CH_2–P), 7.29 (d, 6H, J(H,H) = 8.0 Hz; C_6H_4), 7.40 (d, 6H, J(H,H) = 8.0 Hz; C_6H_4), 7.62 (s, 3H; C_6H_3), 7.92–8.15 (m, 24H; Pyr), 8.72 ppm (d, 6H, J(H,H) = 9.0 Hz; Pyr); ^{31}P{^{1}H} NMR (162 MHz, $CDCl_3$, 298 K, relative to 85% H_3PO_4): $\delta = 12.05$ ppm (s, J(Pt,P) = 2365 Hz); IR (KBr disc): $\tilde{\nu} = 2085$(s), 2111(sh), 2205(w) cm^{-1}, ν(C≡C); positive-ion FAB MS: m/z: 2416 $[M+1]^+$; elemental analysis calcd (%) for **10**: C 62.60, H 5.50; found: C 62.46, H 5.39.

[1,3,5-{HC≡CAnC≡C(PEt$_3$)$_2$PtC≡CC$_6$H$_4$C≡C}$_3$C$_6$H$_3$] (11): The procedure was similar to that for **3** except that a large excess of 1,8-diethynylanthracene (252 mg, 1.12 mmol) was used instead of ethynylbenzene and the complex [1,3,5-{Cl(PEt$_3$)$_2$PtC≡CC$_6$H$_4$C≡C}$_3$C$_6$H$_3$] (100 mg, 0.054 mmol) was added dropwise to the solution of 1,8-diethynylanthracene. Subsequent work-up procedures similar to that for **3** followed by column chromatography on silica gel (70–230 mesh) with dichloromethane as the eluent gave the crude **11** as a bright yellow powder. Recrystallization from dichloromethane/*n*-hexane in the absence of light yielded **11** as an analytically pure bright yellow powder: Yield = 73 mg, 56%; ^{1}H NMR (400 MHz, $CDCl_3$, 298 K, relative to Me_4Si): $\delta = 1.27$ (vq, $J =$ 5.0 Hz, 54H; CH_3), 2.17–2.26 (m, 36H; CH_2–P), 3.47 (s, 3H; C≡CH), 7.28 (d, 6H, J(H,H) = 9.0 Hz; C_6H_4), 7.38–7.42 (m, 12H; 3-An, 6-An and C_6H_4), 7.52 (d, 3H, J(H,H) = 9.0 Hz; 4-An), 7.62 (s, 3H; C_6H_3), 7.74 (d, 3H, J(H,H) = 9.0 Hz; 5-An), 7.80 (d, 3H, J(H,H) = 9.0 Hz; 2-An), 8.01 (d, 3H, J(H,H) = 9.0 Hz; 7-An), 8.40 (s, 3H; 10-An), 9.56 ppm (s, 3H; 9-An); ^{31}P{^{1}H} NMR (162 MHz, $CDCl_3$, 298 K, relative to 85% H_3PO_4): $\delta = 11.82$ ppm (s, J(Pt,P) = 2365 Hz) IR (KBr disc): $\tilde{\nu} = 2085$(s), 2153(w), 2208(w) cm^{-1}, ν(C≡C); positive ion FAB MS: m/z: 2421 $[M+1]^+$; elemental analysis calcd (%) for **11**: C 62.60, H 5.50; found: C 62.66, H 5.55.

[1,3-{PyrC≡C(PEt$_3$)$_2$PtC≡CC$_6$H$_4$C≡C}$_2$-5-{(*i*Pr)$_3$SiC≡C}C$_6$H$_3$] (12): The procedure was similar to that for **10** except that **2** (163 mg, 0.11 mmol) was used instead of **1** to afford **12** as a yellow powder: Yield = 126 mg, 63%; ^{1}H NMR (400 MHz, $CDCl_3$, 298 K, relative to Me_4Si): $\delta = 1.15$ (s, 21H; *i*Pr), 1.29 (vq, $J = 5.0$ Hz, 36H; CH_3), 2.22–2.30 (m, 24H; CH_2–P), 7.28 (d, 4H, J(H,H) = 9.0 Hz; C_6H_4), 7.39 (d, 4H, J(H,H) = 9.0 Hz; C_6H_4), 7.56 (d, 2H, J(H,H) = 1.5 Hz; C_6H_3), 7.62 (t, 1H, J(H,H) = 1.5 Hz; C_6H_3), 7.94–8.14 (m, 16H; Pyr), 8.72 ppm (d, 2H, J(H,H) = 11.0 Hz; Pyr); ^{31}P{^{1}H} NMR (162 MHz, $CDCl_3$, 298 K, relative to 85% H_3PO_4): $\delta =$ 11.75 ppm (s, J(Pt,P) = 2365 Hz) ppm; IR (KBr disc): $\tilde{\nu} = 2086$(s), 2153(w), 2209(w) cm^{-1}, ν(C≡C); positive-ion FAB MS: m/z: 1818

$[M+1]^+$; elemental analyses calcd (%) for **12**: C 64.08, H 6.10; found: C 64.16, H 6.25.

[1,3-{PyrC≡C(PEt$_3$)$_2$PtC≡CC$_6$H$_4$C≡C}$_2$-5-(HC≡C)C$_6$H$_3$] (13): This complex was prepared according to a modified version of a published procedure for the deprotection of the triisopropylsilyl group.[51] nBu$_4$NF (1 mL, 1 M solution in THF) was added to a solution of **12** (25 mg, 0.014 mmol) in THF (15 mL). The reaction mixture was stirred at room temperature for 1 h and was quenched with water. The organic solvent was removed under reduced pressure and the residue was partitioned between dichloromethane and deionized water. The organic phase was dried over anhydrous magnesium sulfate and filtered. Removal of solvent gave the crude product **13** as a yellow powder. Column chromatography on silica gel (70–230 mesh) with dichloromethane/hexane (1:1, v/v) as the eluent gave **13** as a pure pale yellow powder: Yield = 18 mg, 78 %; ^{1}H NMR (400 MHz, $CDCl_3$, 298 K, relative to Me_4Si): $\delta = 1.29$ (vq, $J = 5.0$ Hz, 36H, CH_3), 2.22–2.30 (m, 24H; CH_2–P), 3.11 (s, 1H; C≡CH), 7.28 (d, 4H, J(H,H) = 9.0 Hz; C_6H_4), 7.39 (d, 4H, J(H,H) = 9.0 Hz; C_6H_4), 7.57 (d, 2H, J(H,H) = 1.5 Hz; C_6H_3), 7.65 (t, 1H, J(H,H) = 1.5 Hz; C_6H_3), 7.90–8.14 (m, 16H; Pyr), 8.72 ppm (d, 2H, J(H,H) = 11.0 Hz; Pyr); ^{31}P{^{1}H} NMR (162 MHz, $CDCl_3$, 298 K, relative to 85 % H_3PO_4): $\delta = 11.75$ ppm (s, J(Pt,P) = 2368 Hz); IR (KBr disc): $\tilde{\nu} = 2085$(s), 2155(w), 2211(w) cm^{-1}, ν(C≡C); positive-ion FAB MS: m/z: 1660 $[M+1]^+$; elemental analysis calcd (%) for **13**: C 63.61, H 5.46; found: C 63.82, H 5.52.

[1,8-{Cl(PEt$_3$)$_2$PtC≡C}$_2$An] (14): The procedure was similar to that for **2** except that 1,8-(HC≡C)$_2$An (75 mg, 0.332 mmol) was used instead of 1,3-(HC≡CC$_6$H$_4$C≡C)$_2$-5-{(iPr)$_3$SiC≡C}C$_6$H$_3$. Column chromatography on silica gel with dichloromethane as the eluent gave complex **14** as a bright yellow powder. Subsequent recrystallization from dichloromethane/n-hexane yielded **14** as bright yellow needle-like crystals: Yield = 250 mg, 65 %; ^{1}H NMR (400 MHz, $CDCl_3$, 298 K, relative to Me_4Si): $\delta = 1.24$ (vq, $J = 8.0$ Hz, 36H; CH_3), 2.10–2.20 (m, 24H; CH_2–P), 7.32 (dd, 2H, J(H,H) = 9.0 Hz, 9.0 Hz; 3-An and 6-An), 7.45 (d, 2H, J(H,H) = 9.0 Hz; 4-An and 5-An), 7.79 (d, 2H, J(H,H) = 9.0 Hz; 2-An and 7-An), 8.34 (s, 1H; 10-An) , 9.41 ppm (s, 1H; 9-An); ^{31}P{^{1}H} NMR (162 MHz, $CDCl_3$, 298 K, relative to 85 % H_3PO_4): $\delta = 14.25$ ppm (s, J(Pt,P) = 2393 Hz); IR (KBr disc): $\tilde{\nu} = 2106$(s) cm$^-$, ν(C≡C); positive-ion FAB MS: m/z: 1158 $[M+1]^+$; elemental analysis calcd (%) for **14**: C 43.46, H 5.92; found: C 43.62, H 6.11.

Physical measurements and instrumentation: ^{1}H NMR spectra were recorded on Bruker DPX 300 (300 MHz) or Bruker DPX 400 (400 MHz) Fourier-transform NMR spectrometers with chemical shifts reported relative to tetramethylsilane, Me_4Si, while ^{13}C{^{1}H} and ^{31}P{^{1}H} spectra were recorded on either a Bruker DPX 400 or a Bruker DPX 500 Fourier-transform NMR spectrometer with chemical shifts reported relative to Me_4Si and 85 % H_3PO_4, respectively. Positive-ion FAB mass spectra were recorded on a Finnigan MAT95 mass spectrometer. IR spectra were obtained by using KBr disks on a Bio-Rad FTS-7 Fourier-transform infrared spectrophotometer (4000–400 cm^{-1}). Elemental analyses were performed on a Carlo Erba 1106 elemental analyzer at the Institute of Chemistry, Chinese Academy of Sciences. The electronic absorption spectra were obtained by using a Hewlett–Packard 8452 A diode array spectrophotometer. Steady-state excitation and emission spectra recorded at room temperature and at 77 K were recorded on a Spex Fluorolog-2 Model F111 fluorescence spectrofluorometer. Solid-state photophysical studies were carried out with solid samples contained in a quartz tube inside a quartz-walled Dewar flask. Measurements of the ethanol/methanol (4:1, v/v) glass or solid-state samples at 77 K were similarly conducted by using liquid nitrogen filled in the optical Dewar flask. All solutions for photophysical studies were degassed on a high-vacuum line in a two-compartment cell consisting of a 10 mL Pyrex bulb and a quartz cuvette (1 cm pathlength) and sealed from the atmosphere by a Bibby Rotaflo HP6 Telflon stopper. The solutions were rigorously degassed with at least four successive freeze–pump–thaw cycles. Emission lifetime measurements were performed by using a conventional laser system. The excitation source used was with a 355 nm output (third harmonic) from a Spectra-Physics Quanta-Ray Q-switched GCR-150–10 pulsed Nd-YAG laser. Luminescence decay signals were detected by a Hamamatsu R928 PMT apparatus, recorded on a Tektronix Model TDS-620 A (500 MHz, 2 GS s^{-1}) digital oscilloscope, and analyzed by using a program for exponential fits. Cyclic voltammetric measurements were performed by using a CH Instruments, Inc., model CHI 750 A electrochemical analyzer. Electrochemical measurements were performed in dichloromethane solutions with 0.1 M nBu$_4$NPF$_6$ (TBAH) as the supporting electrolyte at room temperature. The reference electrode was an Ag/AgNO$_3$ (0.1 M in acetonitrile) electrode and the working electrode was a glassy carbon electrode (CH Instruments, Inc.) with a platinum wire as the counter electrode. The working electrode surface was first polished with 1 mm alumina slurry (Linde) on a microcloth (Buehler Co.). It was then rinsed with ultrapure deionized water and sonicated in a beaker containing ultrapure water for five minutes. The polishing and sonicating steps were repeated twice and then the working electrode was finally rinsed under a stream of ultrapure deionized water. The ferrocenium/ferrocene couple ($FeCp_2^{+/0}$) was used as the internal reference. All solutions for electrochemical studies were deaerated with prepurified argon gas prior to measurements.

X-ray crystal structure determination: Crystals of **4** were obtained by layering of n-hexane onto a concentrated dichloromethane solution of the complex. Crystal data: $[C_{99}H_{126}O_3P_6Pt_3]$; formula weight = 2135.09, triclinic, space group $P\bar{1}$ (no. 2), $a = 13.296(3)$, $b = 16.894(3)$, $c = 23.088(5)$ Å, $\alpha = 108.23(3)$, $\beta = 96.20(3)$, $\gamma = 93.33(3)°$, $V = 4873.7(18)$ Å^3, $Z = 2$, $\rho_{calcd} = 1.455$ g cm^{-3}, $\mu(Mo_{K\alpha}) = 4.439$ mm^{-1}, $F(000) = 2136$, $T = 253$ K. A crystal of dimensions $0.5 \times 0.4 \times 0.3$ mm mounted in a glass capillary was used for data collection at 253 K on a MAR diffractometer with a 300 mm image-plate detector and with graphite monochromatized $Mo_{K\alpha}$ radiation ($\lambda = 0.71073$ Å). Data collection was made with 2° oscillation step of ϕ, 600 s exposure time, and scanner distance at 120 mm. 100 images were collected. The images were interpreted and the intensities integrated by using the DENZO program.[52] The structure was solved by direct methods by employing the SIR-97[53] program on a PC. Pt, P, and many non-hydrogen atoms were located according to direct methods and the successive least-squares Fourier cycles. Positions of other non-hydrogen atoms were found after successful refinement by full-matrix least-squares with the SHELXL-97[54] program on a PC. Some Et groups of triethylphosphines were disordered into two different positions. Restraints were applied to the triethylphosphines, with the assumption of similar 1,2- and 1,3-P–C bond lengths within each phosphine, respectively. For one disordered Et group restraints were also applied to assume the same displacement parameters for the disordered parts, respectively. According to the SHELXL-97 program,[54] all 16029 independent reflections (R_{int} equal to 0.0473, 10524 reflections larger than $4\sigma(F_o)$, where $R_{int} = \Sigma|F_0^2 - F_0^2(\text{mean})|/\Sigma[F_0^2]$) from a total of 32691 reflections participated in the full-matrix least-squares refinement against F^2. These reflections were in the range $-15 \le h \le 15$, $-20 \le k \le 20$, $-27 \le l \le 26$ with $2\theta_{max}$ equal to 50.76°. One crystallographic asymmetric unit consisted of one formula unit. In the final stage of the least-squares refinement, carbon atoms of triethylphosphines were refined isotropically, other non-hydrogen atoms were refined anisotropically. The hydrogen atoms were generated by the SHELXL-97[54] program, were calculated based on the riding model with thermal parameters equal to 1.2 times that of the associated carbon atoms, and participated in the calculation of final R indices. Since the structure refinements were against F^2, R indices based on F^2 were larger than (more than double) those based on F. For comparison with older refinements based on F and an OMIT threshold, a conventional index R_1 based on observed F values larger than $4\sigma(F_o)$ was also given (corresponding to Intensity $\ge 2\sigma(I)$). $wR_2 = \{\Sigma[w(F_0^2 - F_c^2)^2]/\Sigma[w(F_0^2)^2]\}^{1/2}$, $R_1 = \Sigma||F_0| - |F_c||/\Sigma|F_0|$. The goodness of fit (GoF) is based on F^2: $\text{GoF} = S = \{\Sigma[w(F_0^2 - F_c^2)^2]/(n-p)\}^{1/2}$, where n is the number of reflections and p is the total number of parameters refined. The weighting scheme is: $w = 1/[\sigma^2(F_0^2) + (aP)^2 + bP]$, where P is $[2F_c^2 + \text{Max}(F_0^2, 0)]/3$. Convergence $((\Delta/\sigma)_{max} = 0.001$, av. 0.001) for 799 variable parameters by full-matrix least-squares refinement on F^2 reaches to $R_1 = 0.0507$ and $wR_2 = 0.1372$ with a goodness-of-fit of 0.993; the parameters a and b for the weighting scheme are 0.0788 and 0. The final difference Fourier map shows maximum rest peaks and holes of 2.064 (near the Pt atom) and -1.321 eÅ^{-3} respectively. Selected bond lengths and angles are summarized in Table 1.

Crystals of **14** were obtained by layering of *n*-hexane onto a concentrated dichloromethane solution of the complex. Crystal data: $[C_{42}H_{68}Cl_2P_4Pt_2]$; formula weight = 1157.92, monoclinic, space group C2/c, $a = 26.705(5)$, $b = 12.999(3)$, $c = 13.953(3)$ Å, $\beta = 101.30(3)°$, $V = 4749.7(16)$ Å^3, $Z = 4$, $\rho_{calcd} = 1.619$ g cm^{-3}, $\mu(Mo_{K\alpha}) = 6.158$ mm^{-1}, $F(000) = 2280$, $T = 253$ K. A crystal of dimensions $0.6 \times 0.3 \times 0.12$ mm mounted in a glass capillary was used for data collection at 253 K on a MAR diffractometer with a 300 mm image plate detector and with graphite-monochromatized $Mo_{K\alpha}$ radiation ($\lambda = 0.71073$ Å). Data collection was made with 2° oscillation step of ϕ, 600 s exposure time, and scanner distance at 120 mm. 100 images were collected. The images were interpreted and intensities integrated by using the DENZO program.[52] The structure was solved by direct methods by employing the SIR-97[53] program on a PC. Pt, Cl, P, and many non-hydrogen atoms were located according to direct methods and the successive least-squares Fourier cycles. Positions of other non-hydrogen atoms were found after successful refinement by full-matrix least-squares by using the SHELXL-97[54] program on a PC. According to the SHELXL-97 program,[54] all 4159 independent reflections (R_{int} equal to 0.0539, 2600 reflections larger than $4\sigma(F_0)$, where $R_{int} = \Sigma|F_0^2 - F_0^2(\text{mean})|/\Sigma[F_0^2]$) from a total 12461 reflections participated in the full-matrix least-square refinement against F^2. These reflections were in the range $-31 \le h \le 31$, $-15 \le k \le 15$, $-15 \le l \le 15$ with $2\theta_{max}$ equal to 50.98°. One crystallographic asymmetric unit consisted of a half formula unit. In the final stage of the least-squares refinement, all non-hydrogen atoms were refined anisotropically. The hydrogen atoms were generated by the SHELXL-97[54] program, were calculated based on the riding model with thermal parameters equal to 1.2 times that of the associated carbon atoms, and participated in the calculation of final *R* indices. Since the structure refinements were against F^2, *R* indices based on F^2 were larger than (more than double) those based on *F*. For comparison with older refinements based on *F* and an OMIT threshold, a conventional index R_1 based on observed *F* values larger than $4\sigma(F_0)$ was also given (corresponding to Intensity $\le 2\sigma(I)$). $wR_2 = \{\Sigma[w(F_0^2 - F_c^2)^2]/\Sigma[w(F_0^2)^2]\}^{1/2}$, $R_1 = \Sigma||F_0| - |F_c||/\Sigma|F_0|$. The goodness of fit (GoF) is always based on F^2: $\text{GoF} = S = \{\Sigma[w(F_0^2 - F_c^2)^2]/(n-p)\}^{1/2}$, where *n* is the number of reflections and *p* is the total number of parameters refined. The weighting scheme is: $w = 1/[\sigma^2(F_0^2) + (aP)^2 + bP]$, where *P* is $[2F_c^2 + \text{Max}(F_0^2, 0)]/3$. Convergence $((\Delta/\sigma)_{max} = 0.001$, av. 0.001) for 227 variable parameters by full-matrix least-squares refinement on F^2 reaches to $R_1 = 0.0525$ and $wR_2 = 0.1325$ with a goodness-of-fit of 0.913; the parameters *a* and *b* for the weighting scheme are 0.0907 and 0. The final difference Fourier map shows maximum rest peaks and holes of 2.462 (near the Pt atom) and -3.005 eÅ^{-3}, respectively. Selected bond lengths and angles are summarized in Table 1. CCDC-248964 (**4**) and CCDC-248965 (**14**) contain the supplementary crystallographic data for this paper. These data can be obtained free of charge from The Cambridge Crystallographic Data Centre via www.ccdc.cam.ac.uk/data_request/cif.

Acknowledgements

V.W.-W.Y. acknowledges support from The University of Hong Kong Foundation for Educational Development and Research Limited. The work described in this paper has been supported by a CERG grant from the Research Grants Council of the Hong Kong Special Administrative Region, China (Project No.: HKU 7123/00P). C.-H.T. acknowledges the receipt of a Croucher Scholarship, a Li Po Chun Postgraduate Scholarship, and a Sir Edward Youde Memorial Fellowship, administered by the Croucher Foundation, the Li Po Chun Charitable Fund, and the Sir Edward Youde Memorial Fund Council, respectively.

[1] R. S. Knox in *Primary Processes of Photosynthesis, Vol. 2* (Ed.: J. Barber), Elsevier, Amsterdam, **1977**.
[2] B. Deming-Adams, *Biochim. Biophys. Acta* **1990**, *1020*, 1.
[3] A. Adronov, J. M. J. Fréchet, *Chem. Commun.* **2000**, 1701–1710, and references therein.
[4] M. Lor, J. Thielemans, L. Viaene, M. Cotlet, J. Hofkens, T. Weil, C. Hampel, K. Müllen, J. W. Verhoeven, M. van der Auweraer, F. C. De Schryver, *J. Am. Chem. Soc.* **2002**, *124*, 9918–9925.
[5] S. Setayesh, A. C. Grimsdale, T. Weil, V. Enkelmann, K. Müllen, F. Meghdadi, E. J. W. List, G. Leising, *J. Am. Chem. Soc.* **2001**, *123*, 946–953.
[6] A. W. Freeman, S. C. Koene, P. R. L. Malenfant, M. E. Thompson, J. M. J. Fréchet, *J. Am. Chem. Soc.* **2000**, *122*, 12385–12386.
[7] P. Furuta, J. Brooks, M. E. Thompson, J. M. J. Fréchet, *J. Am. Chem. Soc.* **2003**, *125*, 13165–13172.
[8] P. W. Pang, Y. J. Liu, C. Devadoss, P. Bharathi, J. S. Moore, *Adv. Mater.* **1996**, *8*, 237–241.
[9] D. Ma, J. M. Lupton, I. D. W. Samuel, S. C. Lo, P. L. Burn, *Appl. Phys. Lett.* **2002**, *81*, 2285–2287.
[10] C. Devadoss, P. Bharathi, J. S. Moore, *J. Am. Chem. Soc.* **1996**, *118*, 9635–9644.
[11] P. Bhyrappa, J. K. Young, J. S. Moore, K. S. Suslick, *J. Am. Chem. Soc.* **1996**, *118*, 5708–5711.
[12] P. Bhyrappa, J. K. Young, J. S. Moore, K. S. Suslick, *J. Mol. Catal.* **1996**, *113*, 109–116.
[13] A. Miedaner, C. J. Curtis, R. M. Barkley, D. L. DuBois, *Inorg. Chem.* **1994**, *33*, 5482–5490.
[14] J. Losada, I. Cuadrado, M. Moran, C. M. Casado, B. Alonso, M. Barranco, *Anal. Chim. Acta* **1997**, *338*, 191–198.
[15] D. Astruc, *Acc. Chem. Res.* **2000**, *33*, 287–298.
[16] M. Albrecht, R. A. Gossage, M. Lutz, A. L. Spek, G. van Koten, *Chem. Eur. J.* **2000**, *6*, 1431–1445.
[17] *Dendrimers and Dendrons: Concepts, Syntheses and Applications* (Eds.: G. R. Newkome, C. N. Moorefield, F. Vögtle), Wiley-VCH, Weinheim, **2001**, pp. 457–537, and references therein.
[18] S. Leininger, P. J. Stang, S. Huang, *Organometallics* **1998**, *17*, 3981–3987.
[19] N. Ohshiro, F. Takei, K. Onitsuka, S. Takahashi, *J. Organomet. Chem.* **1998**, *569*, 195–202.
[20] Y. Liu, S. Jiang, K. Glusac, D. H. Powell, D. F. Anderson, K. S. Schanze, *J. Am. Chem. Soc.* **2002**, *124*, 12412–12413.
[21] S. J. Davies, B. F. G. Johnson, M. S. Khan, J. Lewis, *J. Chem. Soc. Chem. Commun.* **1991**, 187–188.
[22] B. F. G. Johnson, A. K. Kakkar, M. S. Khan, J. Lewis, A. E. Dray, R. H. Friend, F. Wittman, *J. Mater. Chem.* **1991**, *1*, 485–486.
[23] M. S. Khan, A. K. Kakkar, N. J. Long, J. Lewis, P. R. Raithby, P. Nguyen, T. B. Marder, F. Wittmann, R. H. Friend, *J. Mater. Chem.* **1994**, *4*, 1227–1232.
[24] D. Beljonne, H. F. Wittmann, A Köhler, S. Graham, M. Younus, J. Lewis, P. R. Raithby, M. S. Khan, R. H. Friend, J. L. Brédas, *J. Chem. Phys.* **1996**, *105*, 3868–3877.
[25] N. Chawdhury, A. Köhler, R. H. Friend, M. Younus, N. J. Long, P. R. Raithby, J. Lewis, *Macromolecules* **1998**, *31*, 722–727.
[26] N. Chawdhury, A. Köhler, R. H. Friend, W. Y. Wong, J. Lewis, M. Younus, P. R. Raithby, T. C. Corcoran, M. R. A. Al-Mandhary, M. S. Khan, *J. Chem. Phys.* **1999**, *110*, 4963–4970.
[27] V. W. W. Yam, *Acc. Chem. Res.* **2002**, *35*, 555–563, and references therein.
[28] V. W. W. Yam, W. Y. Lo, C. H. Lam, W. K. M. Fung, K. M. C. Wong, V. C. Y. Lau, N. Zhu, *Coord. Chem. Rev.* **2003**, *245*, 39–47.
[29] K. M. C. Wong, C. K. Hui, K. L. Yu, V. W. W. Yam, *Coord. Chem. Rev.* **2002**, *229*, 123–132.
[30] V. W. W. Yam, *Chem. Commun.* **2001**, 789–796.
[31] V. W. W. Yam, L. Zhang, C. H. Tao, K. M. C. Wong, K. K. Cheung, *J. Chem. Soc. Dalton Trans.* **2001**, 1111–1116.
[32] V. W. W. Yam, C. H. Tao, L. Zhang, K. M. C. Wong, K. K. Cheung, *Organometallics* **2001**, *20*, 453–459.
[33] D. T. Gryko, C. Clausen, K. M. Roth, N. Dontha, D. F. Bocian, W. G. Kuhr, J. S. Lindsey, *J. Org. Chem.* **2000**, *65*, 7345–7355.
[34] J. M. Tour, *Chem. Rev.* **1996**, *96*, 537–553.
[35] L. Jones II, J. S. Schumm, J. M. Tour, *J. Org. Chem.* **1997**, *62*, 1388–1410.
[36] N. Ohshiro, F. Takei, K. Onitsuka, S. Takahashi, *Chem. Lett.* **1996**, 871–872.

[37] H. Masai, K. Sonogashira, N. Hagihara, *Bull. Chem. Soc. Jpn.* **1971**, *44*, 2226–2228.
[38] L. Sacksteder, E. Baralt, B. A. DeGraff, C. M. Lukehart, J. N. Demas, *Inorg. Chem.* **1991**, *30*, 2468–2476.
[39] C. L. Choi, Y. F. Cheng, C. Yip, D. L. Phillips, V. W. W. Yam, *Organometallics* **2000**, *19*, 3192–3196.
[40] W. M. Kwok, D. L. Phillips, P. K. Y. Yeung, V. W. W. Yam, *Chem. Phys. Lett.* **1996**, *262*, 699–708.
[41] W. M. Kwok, D. L. Phillips, P. K. Y. Yeung, V. W. W. Yam, *J. Phys. Chem. A* **1997**, *101*, 9286–9295.
[42] L. A. Emmert, W. Choi, J. A. Marshall, J. Yang, L. A. Meyer, J. A. Brozik, *J. Phys. Chem. A* **2003**, *107*, 11340–11346.
[43] I. E. Pomestchenko, N. Felix, *J. Phys. Chem. A* **2004**, *108*, 3485–3492.
[44] I. E. Pomestchenko, C. R. Luman, M. Hissler, R. Ziessel, F. N. Castellano, *Inorg. Chem.* **2003**, *42*, 1394–1396.
[45] "The Electrochemistry of Arenes, Styrenes and Arylalkynes": A. J. Savall in *Rodd's Chemistry of Carbon Compounds*, *Vol. 5 (Topical Volumes; Organic Electrochemistry)*, 2nd ed. (Ed.: M. Sainsbury), Elsevier, Amsterdam, **2002**, pp. 167–224.
[46] A. C. Benniston, A. Harriman, D. J. Lawrie, S. A. Rostron, *Tetrahedron Lett.* **2004**, *45*, 2503–2506.
[47] A. M. McDonagh, M. G. Humphrey, M. Samoc, B. Luther-Davies, *Organometallics* **1999**, *18*, 5195–5197.
[48] L. Dellaciana, A. Haim, *J. Heterocycl. Chem.* **1984**, *21*, 607–608.
[49] D. T. Gryko, C. Clausen, K. M. Roth, N. Dontha, D. F. Bocian, W. G. Kuhr, J. S. Lindsey, *J. Org. Chem.* **2000**, *65*, 7345–7355.
[50] H. E. Katz, *J. Org. Chem.* **1989**, *54*, 2179–2183.
[51] K. Onitsuka, M. Fujimoto, N. Ohshiro, S. Takahashi, *Angew. Chem.* **1999**, *111*, 737–739; *Angew. Chem. Int. Ed.* **1999**, *38*, 689–692.
[52] "Processing of X-ray Diffraction Data Collected in Oscillation Mode": Z. Otwinowski, W. Minor in *Methods in Enzymology, Vol. 276: Macromolecular Crystallography, Part A* (Eds.: C. W. Carter, Jr., R. M. Sweet), Academic Press, San Diego, **1997**, pp. 307–326.
[53] "Sir97: a new tool for crystal structure determination and refinement": A. Altomare, M. C. Burla, M. Camalli, G. Cascarano, C. Giacovazzo, A. Guagliardi, A. G. G. Moliterni, G. Polidori, R. Spagna, *J. Appl. Crystallogr.* **1998**, *32*, 115.
[54] G. M. Sheldrick, SHELX97, Programs for Crystal Structure Analysis (Release 97–2), University of Göttingen, Germany.

Received: August 30, 2004
Revised: November 25, 2004
Published online: January 24, 2005

